

UC San Diego

SIO Reference

Title

Radiance distribution as a function of depth in the submarine environment. Part II. Overcast lighting with tables of radiance -K values for both overcast and sunny lighting conditions

Permalink

<https://escholarship.org/uc/item/5vp2b6cb>

Author

Tyler, John E

Publication Date

1960-02-01

Visibility Laboratory
University of California
Scripps Institution of Oceanography
San Diego 52, California

RADIANCE DISTRIBUTION AS A FUNCTION OF DEPTH
IN THE SUBMARINE ENVIRONMENT

Part II. Overcast Lighting

with

Tables of Radiance -K Values for both Overcast and
Sunny Lighting Conditions

John E. Tyler

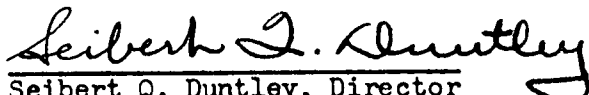
February 1960
Index Number NS 714-100

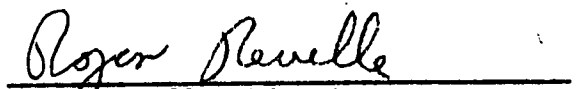
Bureau of Ships
Contract NObs-72092

SIO REFERENCE 60-9

Approved:

Approved for Distribution:


Seibert Q. Duntley, Director
Visibility Laboratory


Roger Revelle, Director
Scripps Institution of Oceanography

RADIANCE DISTRIBUTION AS A FUNCTION OF DEPTH
IN THE SUBMARINE ENVIRONMENT

Part II. Overcast Lighting

with

Tables of Radiance -K Values for both Overcast and
Sunny Lighting Conditions

John E. Tyler

Scripps Institution of Oceanography, University of California
La Jolla, California

ABSTRACT

This report is a continuation of S.I.O. Reference 58-25, entitled
"Radiance Distribution as a Function of Depth in the Submarine Environ-
*
ment." It presents the detailed radiance distribution data obtained
under overcast lighting conditions at the Navy Calibration Station on
Lake Pend Oreille, Idaho, and also gives tables of radiance -K values
for both the overcast and clear-sunny conditions.

* Index No. NS 714-100, 28 March 1958
BuShips Contract No. NObs-72092, Amendment 5

DISCUSSION AND TREATMENT OF DATA FOR OVERCAST CONDITIONS

The diffuse nature of the surface lighting for overcast conditions makes it practical to take data during a longer interval around noon than can be used for the clear sunny sky. For the same reason the order in which the stations are run is far less critical. The near-surface data for overcast sky shows the image features of the barge and its shadow at lower contrast than before. The zenith readings at the near-surface stations may exhibit greater variability in the zenith thickness of the overcast. In addition the generally lower light level puts the deeper stations experimentally beyond reach. Except for these slight differences the experimental procedure was the same for obtaining the overcast data as it was for obtaining clear sunny data.

The overcast data have been treated by the same procedure used for the clear sunny day data as described in (SIO Ref. 58-25) Steps 1 through 9 inclusive with slight modification. Steps 8 and 9 do not, of course, apply as critically to diffuse lighting as they do to the combination of diffuse plus specular lighting provided by a clear sunny day. In Step 6, two complete runs of overcast sky data at each depth station were averaged.

DATA FOR OVERCAST CONDITIONS

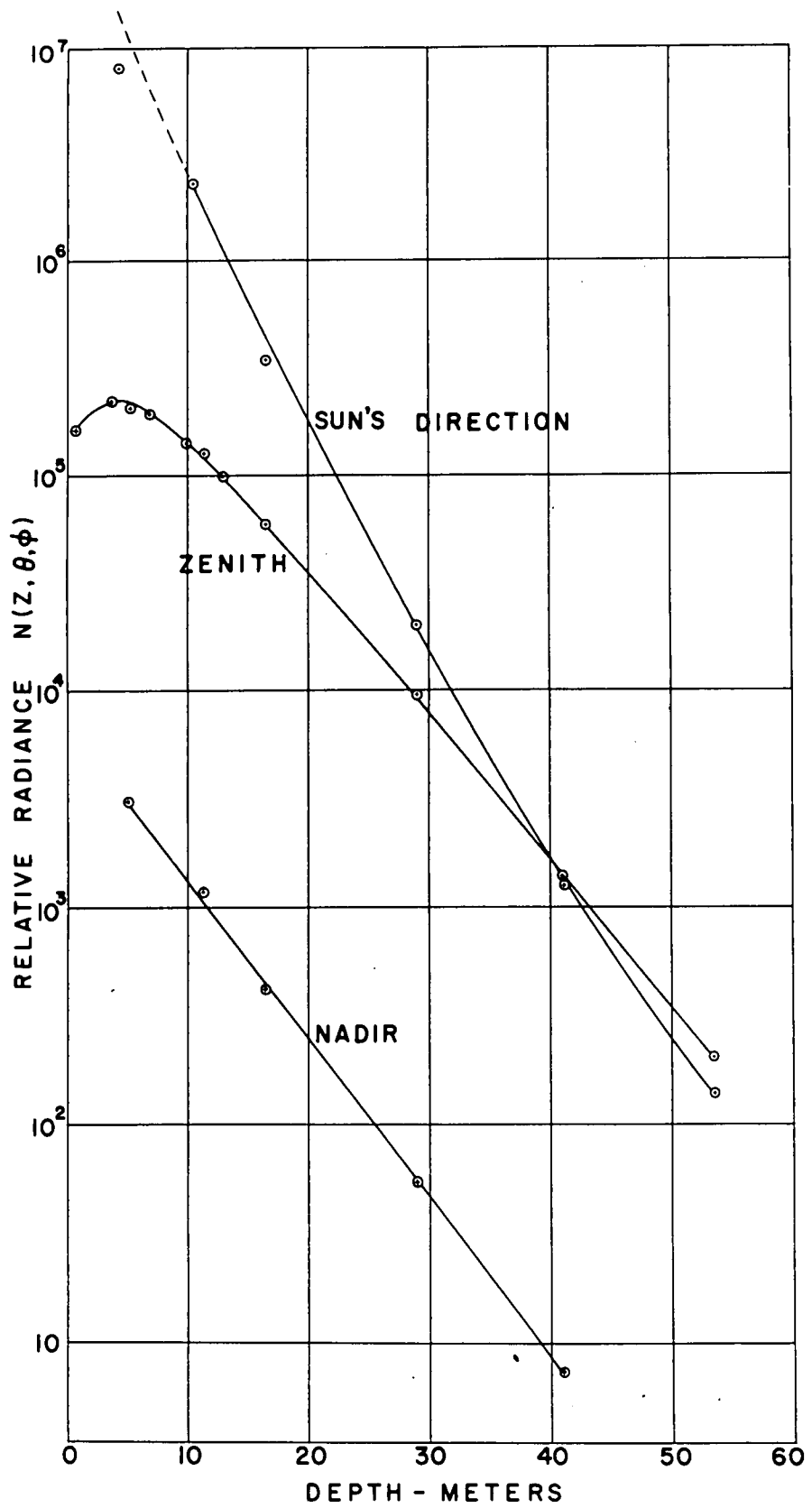
The voice recorded notes for March 16, the overcast day, read in part as follows:

"The data from about 1030 on are all excellent overcast data. The instrument was working perfectly Today's wind velocities ranged from 10 knots at about 1100 to about 2 knots at 1215. At 1400 the water on the south side of the barge where we are operating was as nearly calm as I have seen it"

The radiance distribution data for the overcast condition are given for five depth stations in Tables 12 through 16 inclusive.

DISCUSSION OF DATA AND EVALUATION OF SOURCES OF ERROR

The data presented in Tables 12 through 16 are correct to better than $\pm 5\%$ of the listed value at each entry. Noise due to wave action, and excessive errors in the direction of the sun are not manifest in the overcast data.



ASYMPTOTIC RADIANCE DISTRIBUTION

It has long been conjectured and perhaps first clearly stated by Whitney (1941 a.b.) that the radiance distribution in an optically deep and homogeneous hydrosol approaches a characteristic shape with increasing depth. This final distribution is referred to as the asymptotic radiance distribution because of the manner of its approach to the final shape. Recently Preisendorfer (1958 a, b) has developed a proof of the existence of asymptotic radiance distribution which shows that the final shape depends only on the inherent optical properties of the hydrosol, i.e., the volume scattering function and the absorption coefficient. It is independent of the lighting conditions at the surface of the water and of the optical state of the water surface. As the absorption coefficient approaches 0 in a scattering-absorbing medium the asymptotic radiance distribution tends to become a sphere whereas if the scattering coefficient approaches 0 the final shape tends to be a vertical line. In between these limits there will be an infinite variety of prolate surfaces of revolution oriented with the poles along the vertical axis, each are characteristic of the inherent optical properties of a particular hydrosol.

The transformation of radiance distribution from the complex structure found near the surface to its final symmetrical shape at great depth will require enhancement of radiance in some directions, attenuation in others.

This is evident in the data shown in Fig. (7) and to some extent in the tables of radiance data, and can be deduced from theory in the following way. Starting with the equation of transfer for radiance (1) see Preisendorfer (1958).

$$\cos \theta \frac{dN(z, \theta, \varphi)}{dz} = -\alpha(z)N(z, \theta, \varphi) + N_*(z, \theta, \varphi) \quad (1)$$

Figure 7

Radiance as a function of depth in the zenith and nadir directions and in the direction of the sun's image. The attenuation of light is shown by the slope of the curves. For regions of high radiance the attenuation coefficient is large. For regions of low radiance the attenuation coefficient is low, even negative. When asymptotic radiance distribution is reached the slopes in all directions will be the same.

where θ is the angle from the zenith

ϕ is the azimuth angle from the sun

Z is the depth

N is the radiance

α is the total attenuation coefficient

N_* is the path function

dN , N , and N_* are all taken at the same depth (Z) and in the same direction (θ, ϕ).

We note that the attenuation coefficient (K) for radiance for this same depth and direction is by definition

$$K(Z, \theta, \phi) = - \frac{1}{N(Z, \theta, \phi)} \frac{dN(Z, \theta, \phi)}{dZ} \quad (2)$$

Thus

$$\cos \theta K(Z, \theta, \phi) = \alpha(Z) - \frac{N_*(Z, \theta, \phi)}{N(Z, \theta, \phi)} \quad (3)$$

By definition

$$N_*(Z, \theta, \phi) = \int \mathcal{V}(Z, \theta, \phi, \theta', \phi') N(Z, \theta', \phi') d\Omega$$

over all direction

where the volume scattering function \mathcal{V} has direction θ, ϕ for all incident radiance in the direction θ', ϕ' . For shallow depths the sun is by far the most important contribution to N_* and we can let θ', ϕ' describe the incident radiance from the sun only, that is

$$\begin{aligned} \theta' &= \theta_S \\ \phi' &= \phi_S \\ N &= N_S \\ \Omega &= \Omega_S \end{aligned}$$

When $N_*(Z, \theta, \phi)$ may be approximated by the equation

$$N_*(Z, \theta, \phi) = \sigma(Z, \theta, \phi, \theta_S, \phi_S) N_S \Omega_S \tag{4}$$

Equation (3) can thus be written

$$K(Z, \theta, \phi) \approx \frac{1}{\cos \theta} \left[\alpha(Z) - \frac{\sigma(Z, \theta, \phi, \theta_S, \phi_S) N_S \Omega_S}{N(Z, \theta, \phi)} \right] \tag{4}$$

For the three directions illustrated in Fig. 7 specific values of θ and ϕ can be assigned as shown below; and the negative slopes, K , of the curves of Fig. 7 can be roughly predicted for a fixed depth Z near the surface by equations 5, 6, and 7.

	θ	ϕ	$N(Z, \theta, \phi)$	$(Z, \theta, \phi, \theta_S, \phi_S)$
Zenith	0	0	N_{Zenith}	24° forward scattering = σ_{24}
Sun	θ_S	ϕ_S	N_{Sun}	forward scattering within the beam = σ_0
Nadir	π	0	N_{Nadir}	156° backward scattering = σ_{156}

(The underwater angle of the sun from the zenith (θ_S) for the data presented in this report is about 24°).

$$K_{\text{Zenith}} = \alpha - \frac{\sigma_{24} N_s \Omega_s}{N_{\text{Zenith}}} \quad (5)$$

$$K_{\text{Sun}} = \frac{1}{\cos \theta_s} \left[\alpha - \frac{\sigma_0 N_s \Omega_s}{N_s} \right] \quad (6)$$

$$K_{\text{Nadir}} = - \left[\alpha - \frac{\sigma_{156} N_s \Omega_s}{N_{\text{Nadir}}} \right] \quad (7)$$

It can be seen from Equation 5 that when N_{Zenith} is sufficiently dark, as it is when seen from a depth of less than 4 meters at Lake Pend Oreille on a clear sunny day, the second terms on the right of the equation will be larger than α and a positive slope will result in Fig. 7. With increasing depth N_{Zenith} increases until the two terms on the right of Equation 5 are equal and the slope becomes zero.

In the direction of the sun (Equation 6) the second term on the right of the equation will be minimized due to the presence of N_s in the denominator. The slope in Fig. 7 will therefore be negative and maximized near the surface as shown but will become smaller as N_s decreased with depth.

In the Nadir direction (Eq. 7) the second term will always be larger than ∞ but the change in sign insures that the slope of the curve in Fig. 7 will always be negative. Also since the ratio N_S/N_{Nadir} will not change greatly with depth, the value of K would be expected to remain nearly constant.

From this brief example the usefulness of radiance K data in following and predicting the changes in shape of the radiance distribution solid as a function of depth can easily be seen. By means of radiance K data the radiance distribution at other depths can be easily extrapolated and a quantitative estimate of the proximity to asymptotic distribution can be obtained.

Radiance K data per meter for clear sunny conditions are given in tables 17 through 23 and for overcast conditions in tables 24 through 28.

